Energy & Environmental Science

Cite this: *Energy Environ. Sci.*, 2011, **4**, 4155

www.rsc.org/ees

PAPER

Combining alloy scattering of phonons and resonant electronic levels to reach a high thermoelectric figure of merit in PbTeSe and PbTeS alloys†

Christopher M. Jaworski,[a] Bartlomiej Wiendlocha,[ab] Vladimir Jovovic[a] and Joseph P. Heremans*[ac]

Received 5th June 2011, Accepted 14th July 2011
DOI: 10.1039/c1ee01895g

The effect of the resonant impurity Tl, known to produce a high thermoelectric figure of merit in PbTe through a distortion of the density of states (DOS), is explored here in *p*-type $PbTe_{1-x}S_x$ and $PbTe_{1-y}Se_y$ alloys with direct substitution of Tl for Pb, with the goal of combining its effect with a reduction of the thermal conductivity by alloy scattering. In $PbTe_{1-x}S_x$, the high DOS of PbTe:Tl (x = 0) is maintained up to x = 0.08, whereas the samples' mobility surprisingly increases monotonically with *x*. An optimal composition is found to reach $zT = 1.6$ at x = 0.08, using double-doping with both Tl and Na. The DOS of all $PbTe_{1-y}Se_y$ alloys decreases with y > 0. KKR-CPA electronic structure calculations were performed to enlighten the experimental trends in transport properties: thallium triggers the formation of free-electron-like excess DOS near Fermi level by coupling a Tl 6s-level to the Te p-levels. We ascribe the loss of resonant behavior to a change in overlap between these two levels due to the decrease of the lattice constant with x and y.

Introduction

It was recently shown[1] that the introduction of thallium as a substitutional impurity for Pb in PbTe distorts the density of states (DOS) of the valence band because Tl is a resonant level. This distortion has an energy dependence predicted earlier[2] to enhance the thermoelectric figure of merit zT if located at the Fermi level (E_F), because it leads to a significant enhancement in the thermoelectric power over that of the parent PbTe material. zT is defined by $zT = TS^2\sigma/\kappa$, where S is the material's Seebeck coefficient or thermopower, $\sigma = 1/\rho$ the electrical conductivity, the inverse of its resistivity, and κ is the thermal conductivity. The product $S^2\sigma$ is the thermoelectric power factor (PF). For an impurity energy level to enhance S, it is necessary but not sufficient that it contributes an enhanced DOS; for example Sb substitution for Te in PbTe:Sb was calculated to increase the DOS in the valence band, yet experimentally did not enhance S.[3] Crucial to the thermopower enhancing effect of the resonant level is the need for it to form energy states that couple to the extended states of the solid: this is the case of Tl in PbTe and of Sn in Bi_2Te_3.[4]

Here, we seek to combine the enhanced PF in PbTe:Tl with a lattice thermal conductivity (κ_L) reduced through alloy scattering of phonons by isoelectronic substitution of S or Se for Te. Thus, we focus on solid solutions of $Pb_{0.98}Tl_{0.02}Te_{1-x}S_x$ with

[a]*Department of Mechanical Engineering, The Ohio State University, Columbus, OH*
[b]*AGH University of Science and Technology, Faculty of Physics and Applied Computer Science, al. A. Mickiewicza 30, 30-059 Krakow, Poland*
[c]*Department of Physics, The Ohio State University, Columbus, OH*

† Electronic supplementary information (ESI) available. See DOI: 10.1039/c1ee01895g

Broader context

PbTe is one of the most studied thermoelectric semiconductors because its alloys have the highest energy conversion efficiency (measured by the figure of merit zT) in the 300 °C to 500 °C range, the temperature of exhaust gases of practical combustion processes, such as the exhaust of car engines after the catalytic converter. The last decade of research in thermoelectrics resulted in nearly a doubling of zT, by reducing the thermal conductivity with nanostructuring. There is a limit to the progress that can be made this way, as the lattice thermal conductivity of bulk solids reaches a minimum at the value of amorphous solids. Research into improving the amount of power a thermoelectric material produces for a given temperature difference, the power factor P, focuses on details of the band structure. Doping binary PbTe with the resonant impurity thallium distorts the band structure in such a way as to increase P; here that study is extended to PbTe-PbSe and PbTe-PbS alloys, and the physical nature of the resonance is explored. Tl being unlikely to be used in large-scale applications, understanding the physics of the phenomena will allow other such dopants to be identified.

$0 \leq x \leq 0.16$ and $Pb_{0.98}Tl_{0.02}Te_{1-y}Se_y$ with $0 \leq y \leq 0.20$. In binary PbTe, Tl was calculated to induce two specific energy levels, a hyper-deep state (HDS) and a deep state (DDS), with the latter being in the upper valence band (UVB) and enhancing the thermopower. The Tl-DDS couples to Te 5*p*-states.[5] Here we investigate its effect, both experimentally and using band structure calculations, as Te is being partially substituted with S/Se. One complication in p-type PbTe alloys is the presence of a lower valence band (LVB), which at the highest temperatures might contribute to the high zT in p-type samples doped solely with Na,[6] an explanation that somewhat contrasts with results that n-type PbTe can reach $zT = 1.4$ without the help of a heavy band:[7] the main factor in those systems is the intrinsically low thermal conductivity of PbTe, which itself may be related to lattice instabilities.[8] The Tl energy level adds DOS to the valence band of PbTe, but there is uncertainty in the literature about the energy at which this happens: numbers cited are about 60 meV below the top of the UVB in PbTe, 200 meV in PbSe, and 100 meV in PbS[9,10] (where it is degenerate with the LVB). Experimentally, these energies appear to vary with the concentration of Tl in the sample and different results are deduced from different experiments (transport, optical or tunneling). Tl substituted for Pb is reported to achieve doping levels of 5×10^{19} cm^{-3} in PbS, 12×10^{19} cm^{-3} in PbSe, and 9×10^{19} cm^{-3} in PbTe, values that do not scale properly with the energy levels reported above. Here, we show that Tl contributes DOS starting almost at the top of the UVB, and that 60 meV is the optimum Fermi energy.

Experiments

Stoichiometric amounts (10–20 g total) of the starting elements (≥5N purity, Alfa Aesar) were loaded into quartz ampoules and were sealed under vacuum of 10^{-6} torr or less. PbS containing material ($x \geq 0$) was heated to 1273 K for no more than 6 h, and then annealed for 24–48 h at 1100 K, which is in the single phase region,[11] and then rapidly cooled to 300 K. One sample was double-doped with both 2% Tl and 1% Na substituted for Pb. PbSe containing materials ($y > 0$) were heated to 1273 K for 4 h, rocked, and then rapidly cooled to 773 K for a 7 day anneal. PbTe-PbSe forms a complete solid solution. Powder XRD shows that the materials are single phase and retain cubic symmetry. The lattice spacings closely follow Vegard's law. Following Preier,[12] we assume that the energy gap in $PbTe_{1-x}S_x$ is linear with x, with the 300 K gap of PbTe and PbS reported to be 320 and 410 meV, respectively,[13] whereas the energy gap in $PbTe_{1-y}Se_y$ on the Te rich side remains relatively constant.

Parallelepipeds measuring approximately $1.25 \times 1.25 \times 5$mm^3 were cut using a diamond wire saw for galvanomagnetic and thermomagnetic measurements. Thermopower (S) and transverse adiabatic Nernst-Ettingshausen coefficient were measured using the DC static heater and sink method; the isothermal Nernst coefficient N was calculated from the adiabatic one using a correction factor as described by Tsidil'kovskii.[14] The electrical resistivity (ρ) and Hall coefficient (R_H) were measured using an AC bridge in a 4-wire configuration. We define N and R_H as the low magnetic-field slopes of the transverse Nernst voltages and Hall resistances, respectively. Electrical measurements are taken in a conventional flow cryostat stepping fields from −1.4–1.4 Tesla and temperature from 80–420 K. S and ρ measurements are extended to higher temperature for several samples. Errors on S are limited to better than 3% by the difficulty of measuring the voltage and temperature at exactly the same location. To minimize heat loss, we use 25.4 μm diameter copper and constant wires, which function as type-T thermocouples. The same copper wires are used for voltage. Errors on N, R_H, and ρ are dominated by inaccuracies in measurements of sample geometry, and we estimate them to be 5% on N and R_H, and 7% for ρ. The thermal conductivity below 250 K was also measured using the static heater-and-sink method and above 300 K using a flash-diffusivity method (Anter Flashline 3000). To deduce κ from the diffusivity measurements, the specific heat C_p values were measured in a Quantum Design PPMS at $T \leq 300$ K. The C_p values aligned quite well with literature at 300 K,[15] therefore we used literature data for the binary at $T > 300$ K with a typical value of 0.153 J/gK at 300 K and 0.162 J/gK at 700 K, and correct for molecular weight in the alloys. The values for κ obtained by the two methods also align well. Thermopower and resistivity measurements above 420 K were made using an Ulvac ZEM-3 system, and again align well with the cryostat data. The overall error in zT is actually dominated by that in the specific heat measurement, and estimated to be on the order of 10 to 15% above 420 K.

Electronic properties of $Pb_{0.98}Tl_{0.02}Te_{1-x}S_x$

Thermopower, ρ, N, and the hole concentration p as calculated assuming $p = 1/R_H q$ are plotted in Fig. 1, where q is the electron charge. While no systematic trend in the magnitude of S is observed with x, S of all samples is approximately linear in T, indicating a single carrier system. N is small, less than −0.7 μV/KT, and negative for all samples, which indicates that acoustic and optical phonon scattering dominate. Samples

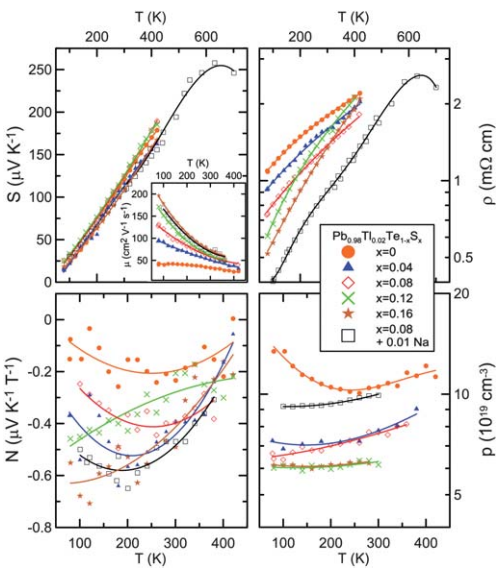

Fig. 1 Thermoelectric properties of sulfur containing materials: Seebeck coefficient (S); electrical resistivity (ρ); Nernst coefficient (N) and carrier concentration (p) for $Pb_{0.98}Tl_{0.02}Te_{1-x}S_x$. Inset: Hall mobility (μ). A sample double doped with Na with S and ρ measured to higher temperature is included. Symbols are experimental points; lines are added to guide the eye.

containing sulfur have lower p than the S-free samples, with p decreasing approximately monotonically with x. All samples with S have lower ρ than the x = 0 sample at T < 400 K, which seems to contradict the observed decrease of p with x; we will show that the hole mobility plays a dominant role. Interestingly, the temperature dependence of ρ for x > 0.08 is different than for x ≤ 0.08. The slight differences between the results at x = 0 and those in ref. 1 are attributed to different material processing techniques: bulk ingots are used here and pressed ball milled material in ref. 1. These have different anneal schedules, which affects the native defect concentration in PbTe and the solubility of Tl in PbTe.

Fig. 2 shows the calculated S *vs.* carrier concentration $S(p)$ or "Pisarenko" relation at 300 K as a full line for the upper valence band (UVB) of PbTe; there is a heavy lower valence band (LVB) which, for instance when reached in Na-doped PbTe[16] at hole doping concentrations $p \sim 5 \times 10^{19}$ cm^{-3}, gives a nearly constant S of S = 50–55 μV/K. As in ref. 1, the samples reported on here have Seebeck coefficients shown as data points in Fig. 2 to be $S \sim 120 \pm 5$ μV/K at 300 K, far above the Pisarenko relation for either LVB or UVB. We conclude that the Tl impurity maintains at least partially its resonant properties up to x = 0.16.

A quantitative analysis is made using the method of the four coefficients described in detail elsewhere,[17] using full Fermi–Dirac statistics. At low temperature, where the Nernst data are less noisy, the four measured transport properties S, N, R_H, and ρ, are used to calculate four unknown material parameters: (1) the Fermi level E_F; (2) the scattering parameter λ defined as the exponent of the energy-dependence of the relaxation time which is assumed to follow a power law $\tau = \tau_0 E^{\lambda}$; (3) the hole mobility μ; and (4) the density-of-states. The latter can be expressed in terms of a density-of-states effective mass m^*, assuming the bands to be locally parabolic at E_F, which is justified by the band structure calculations below and will be discussed there. The DOS and m^* are connected with free-electron-like formula: $DOS = \frac{(m_d^*)^{3/2}}{\pi^2\hbar^3}\sqrt{2E_F}$. Note that the hole density in this method is calculated using E_F and DOS and is more accurate than that determined using $p = 1/R_H q$ as in Fig. 1. Indeed, the method of the four coefficients includes[17] the effect of the Hall prefactor r_H (λ) which describes both the mass anisotropy and the effects of the scattering mechanisms in the formula $p = r_H/R_H q$. In practice, for Tl-doped samples,[18] the difference is of the order of 10 to 20% and does not warrant re-plotting p in a separate figure.

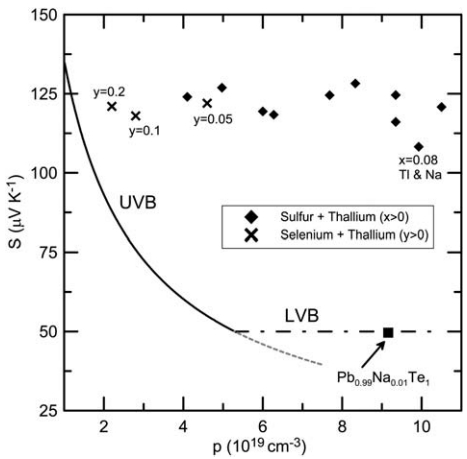

Fig. 2 Pisarenko $S(p)$ relation for p-type PbTe at 300 K: solid and dashed lines are calculated using band effective masses, E_g, and $E_{UVB} - E_{LVB}$, the energy difference between the edges of the UVB and the LVB. The LVB is adapted from 16. The portion (gray dashed line) of the calculated UVB Pisarenko with S below the LVB cannot be realized physically, as carriers will begin to populate the LVB. Unlabeled data points are Tl & S containing samples while Tl & Se samples are labeled with y concentration. We also place a Tl free $Pb_{0.99}Na_{0.01}Te$ sample on this plot.

The results for E_F, λ, DOS or m^* are shown in Table 1, and the following conclusions can be drawn. Most importantly, the DOS at E_F for 2%Tl at x = 0 (0.18 ev^{-1} per formula unit) corresponds very well to the calculated value (0.24 ev^{-1}) below, and to the experimental value (0.3 ev^{-1}) determined from electronic specific heat measurements in a PbTe sample containing 1.4% Tl.[19] It is worth noting that the theoretical DOS calculations below illustrate that a non-parabolic Kane model, which would hold for the UVB, does not apply to the Tl resonant state. Secondly, the value for the scattering exponent $\lambda \sim -0.5$ to 0 (the relative inaccuracy is due to the noise in N, itself due to the fact that the absolute values of both N and λ are very small) indicates that scattering is dominated by acoustic phonons ($\lambda = -0.5$) with a modest contribution of optical phonon ($\lambda = +0.5$), but with no evidence for a resonant scattering mechanism which would lead to $\lambda > 3$ to 4.[20] Also, since resonant scattering is expected only at the lowest temperatures[20] because the effects of phonon scattering increase with temperature, resonant scattering would imply that λ should increase with decreasing temperature, the opposite of what is observed. Thirdly, the calculated E_F (60 ± 10 meV) is nearly constant with S content, indicating a pinned E_F. Fourthly, all samples retain a DOS above that of the UVB of PbTe. In spite of the slightly larger gap of PbS compared to that of PbTe and the concomitant increase of DOS of the UVB with x in the absence of resonant levels, a decrease of DOS with increasing x is observed. Finally, the low-temperature mobility (Fig. 1 inset) improves monotonically with increasing sulfur content, contrary to what is expected from alloy scattering; this latter effect is unexplained.

Electronic properties of $Pb_{0.98}Tl_{0.02}Te_{1-y}Se_y$

Fig. 3 shows ρ, S, N, and p as functions of temperature. All samples have similar S at 80 K < T < 420 K, whereas the S of y > 0 are 10–15% larger at higher T. p is nearly constant over T for all samples and decreases with Se concentration. As in S containing samples, ρ decreases monotonically with increasing y at T < 400 K. However, this inverts at 400 K due to the increased dρ/dT with increased y. N also has a significant dependence on y, which appears to saturate at y ≥ 0.10. As T is increased, the deviation in N for samples with y > 0 is diminished, and reach similar values of N at 400 K. Unfortunately, the large increase at high T in ρ for y > 0 is not compensated by an increased S and thus the power factor drops.

Using the method of four coefficients as above we calculate at 80 K $\lambda \sim -0.5$ for all samples, which lies in agreement with sulfur containing samples, and indicates that the dominant scattering

Table 1 Band structure parameters of $Pb_{0.98}Tl_{0.02}Te_{1-x}S_x$ alloys calculated from the method of the four coefficients (see text). The values for pure PbTe are calculated using the Kane band model for the LVB alone and $E_F = 60$ meV, using published band structure data[21]

Sulfur concentration	E_F(80 K) (meV)	E_F(300 K) (meV)	m^* (80 K) (m_e)	m^* (300 K) (m_e)	λ (80 K)	λ (300 K)	DOS (E_F, 80 K) (eV^{-1} per f.u.)	DOS (E_F, 300 K) (eV^{-1} per f.u.)
Pure PbTe	60	60	0.14	0.17	—	—	0.010	0.012
x = 0%	57	57	1.38	1.33	−0.30	−0.06	0.178	0.168
4%	53	55	1.18	1.18	−0.50	−0.12	0.134	0.137
8%	64	58	0.92	1.12	−0.10	0.00	0.100	0.128
12%	57	66	0.98	0.86	−0.27	0.14	0.103	0.091
16%	48	66	1.25	0.94	−0.56	−0.06	0.135	0.103
8% + 1%Na	66	67	1.06	1.15	−0.24	−0.01	0.126	0.144

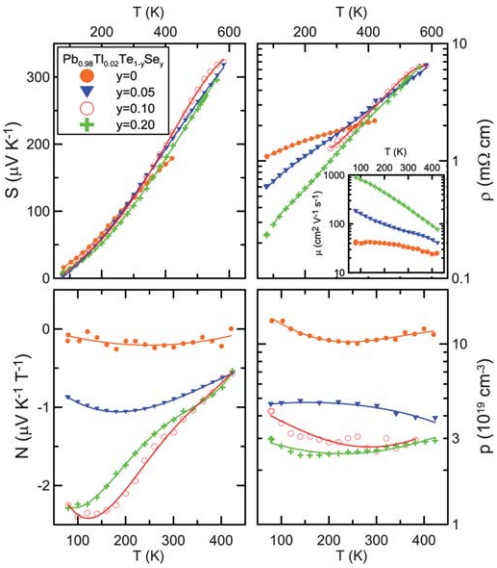

Fig. 3 Thermoelectric properties of Se containing materials: Seebeck coefficient (S); electrical resistivity (ρ); Nernst coefficient (N) and carrier concentration (p) for $Pb_{0.98}Tl_{0.02}Te_{1-y}Se_y$. Inset: Hall mobility (μ). Symbols are experimental points; lines are added to guide the eye.

mechanism is acoustic phonon scattering. Further calculations of E_F and DOS or m^* are shown in Table 2; we can observe that while E_F decreases slightly with y at 300 K, DOS is strongly reduced. As can be observed from the Pisarenko plot (Fig. 2) $S(p, 300\ K)$ remains constant for all alloys, but this is in part explained because p decreases with y. Fig. 2 shows that the range of hole concentrations that can be reached experimentally is much narrower for Se-substituted alloys than for S-substituted ones, presumably due to a different defect chemistry. We will argue later that this, rather than some intrinsic electronic property of the Tl–Se bond, is the main limitation to the use of $Pb_{0.98}Tl_{0.02}Te_{1-y}Se_y$ alloys.

Thermal conductivity and zT

Fig. 4 (top) shows thermal conductivity κ for the samples over temperature. We calculate lattice thermal conductivity κ_L for y > 0 samples (at y = 0 we use the data of ref. 1) by subtracting from κ values of electronic component using $\kappa_e = L\sigma T$, where L is the Lorenz number. While it is possible to use the measured electrical conductivity and the free electron value for $L = L_0$ in

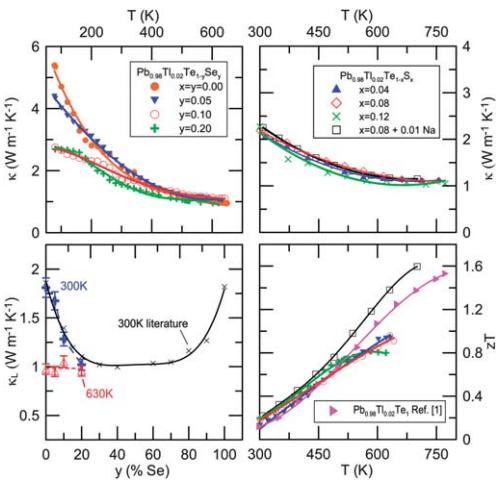

Fig. 4 Thermal conductivity and thermoelectric figure of merit. Top panels: thermal conductivity (κ) *versus* temperature for S and Se compounds. Bottom left panel: calculated κ_L of $Pb_{0.98}Tl_{0.02}Te_{1-y}Se_y$ at 300 K and 630 K and literature values of κ_L of $PbTe_{1-y}Se_y$. Bottom right panel: figure of merit zT for selected samples with the symbols of Fig. 1 or 3. Symbols are experimental points; lines are added to guide the eye.

Table 2 Band structure parameters of $Pb_{0.98}Tl_{0.02}Te_{1-y}Se_y$ alloys calculated from the method of the four coefficients. The values for pure PbTe are from Table 1

Selenium concentration	E_F (80 K) (meV)	E_F (300 K) (meV)	m^* (80 K) (m_e)	m^* (300 K) (m_e)	λ (80 K)	λ (300 K)	L/L_0 300 K	L/L_0 650 K	DOS (E_F, 80 K) (eV^{-1} per f.u.)	DOS (E_F, 300 K) (eV^{-1} per f.u.)
Pure PbTe	60	60	0.14	0.17	—	—	—	—	0.010	0.012
y = 0%	57	57	1.38	1.33	−0.30	−0.06	0.89	0.8	0.178	0.168
5%	70	47	0.66	0.95	-0.9	-0.2	0.9	0.77	0.065	0.091
10%	—	55	—	0.58	—	−0.09	0.86	0.75	—	0.047
20%	88	65	0.4	0.49	-0.6	−0.03	0.87	0.7	0.033	0.039

cases where electron scattering is fully elastic to estimate κ_e, doing so for the narrow-gap semiconductors studied here would result in a gross overestimation of the electronic contribution of thermal conductivity, particularly at high temperatures. Following Ravich,[21] Kolodziejczak,[22] and using the band parameters from the four coefficient method, we calculate the ratios of Lorenz number to free electron Lorenz number as L/L_0 (Table 2). We see that these values can be reduced up to 30%. As shown in Fig. 4c the calculated κ_L follow those of undoped PbTe-PbSe alloys reported in ref. 23. There is no further effect on reduction of thermal conductivity over Tl-free materials and alloy scattering is the dominant phonon scattering process at 300 K. At 630 K, however, Umklapp processes dominate, and the substitution of Se has no observable effect on the lattice thermal conductivity.

Because the best zT is observed in the highest-doped samples, and because Tl has a solubility limit in PbTe, we double doped an $x = 0.08$ sample with 1 at% Na substituted for Pb, and show its electrical properties in Fig. 1. S and ρ are lower than for the other samples due to the increased carrier density and κ is slightly higher (Fig. 4b) due to increased electronic κ_e. We carried out electronic structure calculation like those described below, and they show that Na-doping mainly changes the position of the Fermi level, acting as a simple acceptor without modifying the general shape of DOS near E_F. The zT, (Fig. 4d), reaches 1.6 at 700 K, and illustrates that indeed the positive aspects of resonant levels work independently of the effects of alloy scattering. We have prepared samples with $x = 0.08$ and doped p-type solely with Na, not Tl. These samples exhibit power factors 10–15% lower than samples with Tl at all temperatures; even at 700 K, PF $\sim$ 25-to-26 $\mu W\ K^{-2}cm^{-1}$ in Tl-containing materials *versus* 22-to-23 $\mu W\ K^{-2}cm^{-1}$ in solely Na-doped material. The improvement in peak zT in Tl-containing materials at the highest temperature may not be significantly above the experimental uncertainties and sample-to-sample variations, but the resonant Tl level significantly improves the average zT integrated over T, because it strongly improves the lower-temperature S. These results will be published elsewhere.[24] The zT for of $PbTe_{1-y}Se_y$ alloys ($y > 0$) is lower than that of binary PbTe due to the elevated ρ at high temperature.

Theory and discussion

To enlighten the experimental trends in transport properties, and to elucidate the criteria necessary for resonant levels to enhance zT, electronic structure calculations were performed using the Korringa-Kohn-Rostoker (KKR) Green function method[25,26] with the coherent potential approximation (CPA) used to treat disorder in alloys. The muffin tin type of crystal potential was constructed in the framework of the local density approximation (LDA), using von Barth and Hedin formula for the exchange–correlation part. For all atoms angular momentum cut-off $l_{max} = 3$ was set and semi-relativistic calculations were performed. Both full potential semi-relativistic and full potential, fully relativistic calculations were carried out for binary PbTe in order to check the influence of the spherical potential (muffin tin) approximation and the spin–orbit interaction on the electronic structure of the valence band. High convergence limits were put on the self-consistent cycle (10^{-4}q for charge, 10^{-4} Ry for Fermi level E_F and 10^{-6} Ry for total energy) and all results were checked for convergence against **k**-point number (up to 1800 **k**-points in irreducible part of Brillouin zone); this level of accuracy for the position of E_F was obtained using the generalized Lloyd formula.[27] For the finally convergent potentials, the DOS was computed using the tetrahedron **k**-space integration technique.

Vegard's law was used to obtain the crystal structure data for $PbTe_{1-y}Se_y$ and $PbTe_{1-x}S_x$ alloys by scaling the room temperature lattice. The effects of dynamical instabilities that occur in PbTe[8] and probably in $PbTe_{1-x}S_x$[28] and $PbTe_{1-y}Se_y$[29] alloys were not taken into account. As previously discussed,[5,30,31,32] the band gap in PbTe computed using semi-relativistic treatment is overestimated by a factor of 3 to 4 (we get 0.65 eV). Inclusion of spin orbit interaction lowers the gap significantly and restores the typical LDA gap underestimation (we get 0.11 eV using a full-potential fully relativistic calculation), to be compared to an experimental value of 0.19 eV at 0 K. Improvement using specific LDA-type exchange–correlation potential have been recently reported.[33] A comparison of last valence bands and first conduction band in PbTe obtained in semi relativistic and full-relativistic calculations shows that mainly the position of conduction band is shifted with respect to the valence band, and the DOS close to valence band edge is only slightly modified.† Furthermore, a previous supercell-based theoretical study of Tl impurity in PbTe[5] found that spin–orbit interaction does not change significantly the impurity states. Also, the differences between spherical potential and full-potential results were not significant within the semi-relativistic approximation. For all those reasons, only spherical potential, semi relativistic approximations are used for disordered $Tl:PbTe_{1-x}S_x$ and $Tl:PbTe_{1-y}Se_y$ alloys, and the qualitative conclusions of the calculations are expected to hold.

Moving now to the effect of Se and S substitutions for Te on the resonance of the Tl atoms, the calculated DOS of $x = 0.1$ is shown in Fig. 5. The results (not shown) for $y = 0.1$ are nearly identical. The large-energy-scale effects are similar to those on PbTe:Tl; detailed changes upon S/Se doping are discussed later. The locations of the S 3s and 3p energy bands (or Se 4s and 4p) follow these of corresponding Te 5s and 5p states. As in PbTe case[5,30,31,32] the DOS consists of four separate blocks: two low-lying s-like (5s electrons of Te and 6s of Pb) blocks, and valence and conduction bands (5p-Te and 6p-Pb) separated by the band gap (overestimated in our calculations by semi-relativistic approach). The Tl atoms create three sharp DOS peaks, corresponding to three impurity states typical for group-III elements in the lead salts. First is a semi-core d level (5d in Tl case) located about -10 eV below Fermi level. Second and third are the unusual 6s-like hyper deep (HDS, -5 eV below E_F) and deep (DDS, at E_F) defect states, the latter being the one that influences the thermoelectric properties. The 6p Tl states are built into the valence band block lying between -5 eV and E_F. Our results confirm previous ones on the position and character of deep impurity states obtained from supercell calculations, using FP-LAPW method.[5,30]

Both HDS and DDS states are formed by the interaction of Tl-s and Te-p orbitals, but there is an important difference between them that helps to understand differences in their evolution upon Te/Se and Te/S substitution. The relative contribution to the total DOS of HDS state (calculated as a ratio

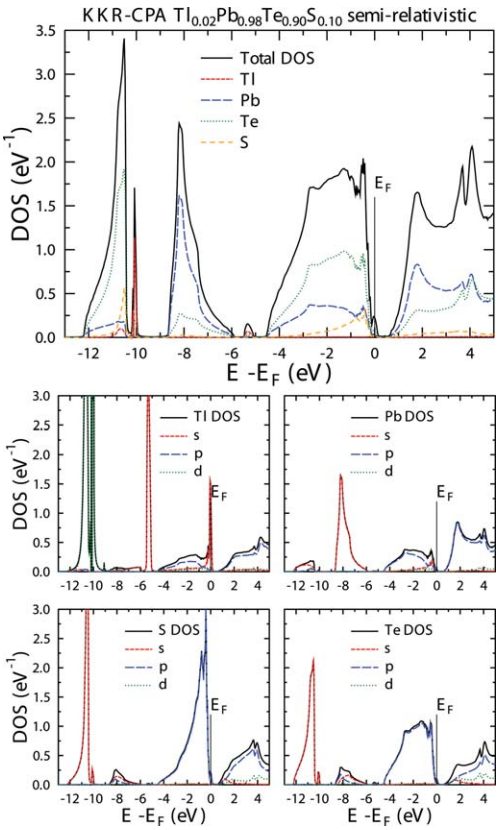

Fig. 5 Density of states of $Pb_{0.98}Tl_{0.02}Te_{0.90}S_{0.10}$. Upper panel: total density of states and atomic contributions weighted by concentration. Lower panels: partial atomic densities of states with angular momentum decomposition.

of partial DOS and total DOS at DOS maximum located at −5.3 eV) from Tl, Te and Pb atoms are about: 46% (Tl), 26% (Te), and 7% (Pb), with the rest coming from interstitial states. For DDS states, these contributions calculated at the Fermi level are 12% (Tl), 50% (Te), and 15%(Pb). Thus, formation of both HDS and DDS is possible only when Tl atoms are present in PbTe, but HDS is more Tl-like and DDS is more Te-like. Because of this, the HDS DOS doesn't change much upon Te/Se or Te/S substitution, while important changes are made for the DDS.

The "hump" in DOS, created by the Tl atoms, is suggestive of the DOS for the "best thermoelectric" concept,[2] where the best material would have a delta-like excess in DOS with as little as possible background DOS; it is such a background that appears with S/Se substitution at higher doping level (see below). This DOS "hump" can be locally fitted† using the square-root dependence on energy, a free-electron-like formula, but with constant and negative factor: $DOS(E) = a \cdot \sqrt{E_V - E} - b$, where $a = 0.84 \pm 0.02$ ($eV^{-3/2}$), $b = 0.1 \pm 0.005$ (ev^{-1}), and E_V is the valence band edge. This observation justifies using the parabolic model for the four coefficients method used above. The value of fitting parameter a corresponds to the effective mass $m^* \approx 1.5\ m_e$, which is close to the value extracted from the four coefficients method ($m^* \approx 1.35 \pm 0.3\ m_e$ for x = 0, see Table 1). Adding Tl to PbTe, in addition to doping it p-type, triggers the formation of resonant-yet-nearly-free-electron-like states, joining two features that are easily but erroneously perceived as contradictory in light of the fact that many resonant levels involve often localized d-electrons.[34] However, one should bear in mind that presence of constant factor b in formula used for fitting partly limits the free-electron interpretation and shows the important effects of crystal potentials.

Using the simplified formula for degenerate bands that ignores the effect of scattering, $S = \frac{\pi^2}{3}\frac{k_B}{q}k_BT\frac{DOS(E_F)}{\int_{E_F}^{E_V} DOS(E)dE}$, one can infer the thermopower from the DOS humps in Fig. 6: 90 μV K^{-1} at 300 K. This value is close to the experimental one (120 μV K^{-1}) in Fig. 2; the agreement can be considered excellent given the assumptions taken, such as neglecting scattering effects.

Let us now concentrate on the evolution of DOS with S/Te substitution. The DOS does not change much for x < 0.1 (Fig. 6a); neither does the calculated Fermi level position with respect to the valence band edge. The distance between E_F and the valence band edge is overestimated (150 meV instead of 60 meV), in line with the overestimation of the gap. The independence of the DOS on x is very consistent with the constancy of the thermopower at 300 K shown in Fig. 2. The changes in DOS are only visible above x = 0.15, where the hump broadens and starts to join the main valence DOS, filling the valley which separated both regions and increasing the density of background states, an unfavorable feature for zT.[2] Calculations (Fig. 6d) don't predict as abrupt a drop in total DOS as is shown in Table 1, but important decreases in partial DOS occur. Fig. 6c presents the evolution of the Tl partial DOS peak (mainly s-like) upon S/Te substitution. Starting at x = 0.15, the DOS broadens, which causes the broadening of the whole DDS DOS, and the DOS at E_F drops significantly for x = 0.2. Fig. 6d shows contributions to total DOS at the Fermi level coming from all the atoms, weighted by their concentrations. The Te contribution

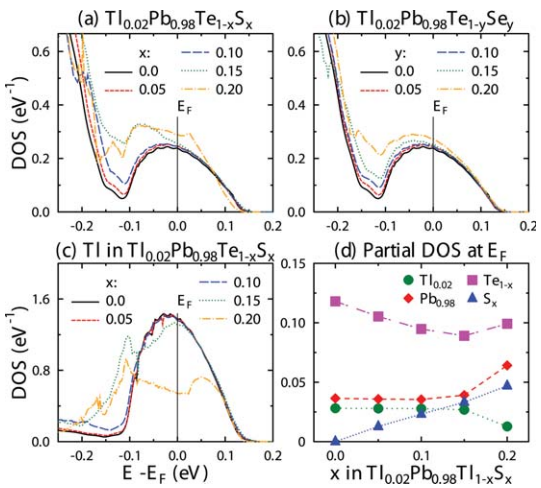

Fig. 6 (a) Evolution of total DOS close to E_F for S-substituted $Pb_{0.98}Tl_{0.02}Te$; (b) Evolution of total DOS close to E_F for Se-substituted $Pb_{0.98}Tl_{0.02}Te$; (c) Evolution of partial DOS of Tl atom (mostly s-like) near E_F in $Pb_{0.98}Tl_{0.02}Te_{1-x}S_x$. Up to x = 0.1, the resonant "hump" is not x-dependent; for x ≥ 15% it is lowered, broadened, and starts to join the main valence DOS; (d) Atomic contributions to total DOS at E_F, weighted by concentrations, in $Pb_{0.98}Tl_{0.02}Te_{1-x}S_x$.

generally decreases with x, and this effect is present even if Te DOS is counted per atom (not multiplied by concentration). Adding the contributions of both Te and S to the DOS shows that the contribution of the S/Te site is constant up to x = 0.15, but for x = 0.2 its value increases (samples with that concentrations could not be synthesized as solid solutions). In summary, the loss of the resonant behavior of Tl observed experimentally for x > 0.08, is related to the broadening of the total and partial Tl-DOS, the decrease in partial (mainly s-like) Tl-DOS and the decrease in partial (mainly p-like) Te DOS.

The calculations for the Se substitutions follow the experiment less well. Transport measurements show a rapid decrease in DOS even at y = 0.05, while in calculations results are qualitatively similar to those of S case (Fig. 6b). For selenium the calculated modifications to DOS are less pronounced and more gradual than for sulfur, which is intuitively understood since Se is chemically more similar to Te than S. We tentatively conclude that the differences in observed experimental results between the PbTeS and PbTeSe systems may be ascribed to their different defect chemistry, which allowed only for a more limited hole concentration and E_F range to be explored in the Se/Te system (Fig. 2).

The fundamental cause for the decreased efficiency of the Tl resonant level in boosting the thermopower as the Te concentration decreases will now be shown to be related to the lattice constant. We computed density of states for 20% Se(S)/Te substitution now ignoring changes in lattice parameter: the characteristic DOS hump was almost unchanged compared to the x,y = 0 case.† This suggests that the decrease in lattice constant with Se or S substitution, rather than the electronegativity of the lighter chalcogens, plays a dominant role, *i.e.* that the effect is due to "chemical pressure"; in this model, the broadening of a thallium partial DOS peak is a pressure-driven enhanced hybridization of Tl s-orbitals with the valence bands of PbTe. The decrease in lattice constant affects the overlap between the Tl 6s states and the Te 5p, and thus the delicate balance between increases in DOS and nearly-free-electron behavior that lies at the origin of the thermopower enhancements. Since changes in lattice parameter made by Se/Te substitution are smaller, the effect made by insertion of Se atoms is expected to be weaker, at least in our spherical-potential semi-relativistic CPA calculations. We also simulated the opposite trend, *i.e.* performed computations for 2%Tl doped PbTe with a hypothetically larger lattice parameter (about 1.5%.) and found increases in both DOS and Seebeck coefficient of about 5%. This finding leaves open the possibility of a further increase in zT of the x > 0 alloys through usage of heat treatments designed to exploit the spinodal decomposition regime,[35] thus reducing thermal conductivity *via* nanostructuring[36] instead of alloy scattering, and optimizing the lattice parameter to maximize the power factor.

Summary

In summary, we show that the distortion in DOS observed in $Pb_{0.98}Tl_{0.02}Te$ is maintained for $Pb_{0.98}Tl_{0.02}Te_{1-x}S_x$ alloys with low S content ($x \leq 0.08$). Tl continues to act as a resonant level, pinning the S at ~120 μV/K at 300 K. The fact that the mobility in these alloys increases with x is surprising and unexplained. For $Pb_{0.98}Tl_{0.02}Te_{1-y}Se_y$ alloys, both carrier density and hole effective mass decrease with y, the Tl resonant level is partially lost, and the samples return to the Pisarenko curve for the UVB of PbTe. In these alloys also, alloy scattering of phonons lowers the thermal conductivity at 300 K as known, but at 600 K this effect is small. Electronic band structure calculations show that thallium 6s-states, coupled with Te 5p ones, create an excess DOS in PbTe that evolves little with Se/Te and S/Te substitution for low concentrations, and dominates the thermopower at 300 K. In Tl-doped PbTe and its alloys, the Tl 6s-states trigger the formation of sharp DOS peaks, a behavior typically associated to more localized 3-d transition metal states, but with a free electron-like local energy dependence $DOS(E) \sim \sqrt{E}$. The decrease in lattice constant with the Se/Te and S/Te substitutions lies at the origin of the smearing out of the Tl level at higher concentrations. The effectiveness of a resonant level in enhancing the thermoelectric power factor depends critically on the amount of overlap between the impurity states and the band structure of the host semiconductor. Too much overlap, induced here by the reduction in lattice constant, decreases the excess in thermopower; too little overlap creates states that are too localized and do not conduct well. The understanding presented here of the role of resonant levels should apply to other semiconductor systems and aid in developing other high-zT thermoelectric alloys.

This work is supported by a sponsored research agreement with ZT::Plus, Azusa, CA. We thank Yibin Gao for useful discussions.

References

1 J. P. Heremans, V. Jovovic, E. S. Toberer, A. Saramat, K. Kurosaki, A. Charoenphakdee, S. Yamanaka and G. J. Snyder, *Science*, 2008, **321**, 554.
2 D. G. Mahan and J. O. Sofo, *Proc. Natl. Acad. Sci. U. S. A.*, 1996, **93** (15), 7436–7439.
3 C. M. Jaworski, J. Tobola, E. M. Levin, K. Schidt-Rohr and J. P. Heremans, *Phys. Rev. B: Condens. Matter Mater. Phys.*, 2009, **80**, 125208.
4 C. M. Jaworski, V. Kulbachinskii and J. P. Heremans, *Phys. Rev. B: Condens. Matter Mater. Phys.*, 2009, **80**, 233201.
5 K. Hoang and S. D. Mahanti, *Phys. Rev. B: Condens. Matter Mater. Phys.*, 2008, **78**, 085111.
6 Y. Pei, A. LaLonde, S. Iwanaga and G. J. Snyder, *Energy Environ. Sci.*, 2011, **4**, 2085–2089.
7 A. D. Lalonde, Y. Pei and G. J. Snyder, *Energy Environ. Sci.*, 2011, **4**, 2090–2096.
8 E. S. Bozin, C. D. Malliakas, P. Souvatzis, T. Proffen, N. A. Spaldin, M. G. Kanatzidis and S. J. L. Billinge, *Science*, 2010, **330**, 1660.
9 Y. I. Ravich and S. A. Nemov, *Phys.-Usp.*, 1998, **41**(8), 735–759.
10 V. I. Kaidanov, S. A. Nemov and Y. I. Ravich, *Sov. Phys. Semicond*, 1992, **26**, 113.
11 A. A. Volkhov, L. V. Yashina and V. I. Shtanov, *Inorg. Mater.*, 2006, **42**, 596–604.
12 H. M. Preier, *Lect. Notes Phys.*, 1982, **152**, 289; *Proceedings of the 4th Int. Conf. on Narrow-Gap Semiconductors*, Linz, (1981).
13 S. Kasimov, A. R. Regel and V. K. Subashie, *Sov. Phys. Solid State, USSR*, 1968, **9**(12), 3653–3654.
14 I. M. Tsidil'kovskii, *Thermomagnetic Effects in Semiconductors*, Academic, New York (1962).
15 R. Blachnik and R. Igel, *Z. Naturforsch., B: Chem. Sci*, 1974, **29**, 625; A. S. Pashinkin, M. S. Mikhailova, A. S. Malkova and V. A. Federov, *Inorg. Mater.*, 2009, **45**, 1226–1229.
16 S. V. Airapetyants, M. N. Vinogradova, I. N. Dubrovskaya, N. V. Kolomoets and I. M. Rudnik, *Sov. Phys. Solid State*, 1966, **8** (5), 1336–1340.
17 J. P. Heremans, C. M. Thrush and D. T. Morelli, *Phys. Rev. B: Condens. Matter Mater. Phys.*, 2004, **70**, 115334.

18 The Hall prefactor is considerably more T-dependant in Na:PbTe [A. J. Crocker and L. M. Rogers, *Br. J. Appl. Phys.*, 1967, **18**, 53] than in Fig. 1c, due to a temperature induced redistribution of holes between the UVB and LVB [see ref. 20 and references therein].
19 Y. Matsushita, P. A. Wianecki, A. T. Sommer, T. H. Geballe and I. R. Fisher, *Phys. Rev. B: Condens. Matter Mater. Phys.*, 2006, **74**, 134512.
20 S. J. Thiagarajan, V. Jovovic, S. West and J. P. Heremans, *Phys. Stat. Sol*, 2007, **1**(6), 256–258.
21 Y. I. Ravich, *Semiconducting Lead Chalcogonides*, Plenum Press, New York, 1970.
22 J. Kolodziejczak and L. Sosnowski, *Acta Phys. Pol.*, 1962, **21**, 399.
23 G. Nimtz & B. Schlicht, *Narrow Gap Semiconductors (Springer Tracts in Modern Physics*, Vol. 98, Ed. G Hohler, Berlin: Spring-er-Verlag, (1983).
24 C. M. Jaworski, *et al.*, in preparation.
25 A. Bansil, S. Kaprzyk, P. E. Mijnarends and J. Tobola, *Phys. Rev. B: Condens. Matter*, 1999, **60**, 13396.
26 T. Stopa, S. Kaprzyk and J. Tobola, *J. Phys.: Condens. Matter*, 2004, **16**, 4921.
27 S. Kaprzyk and A. Bansil, *Phys. Rev. B: Condens. Matter*, 1990, **42**, 7358.
28 Z. Wang and B. A. Bunker, *Phys. Rev. B: Condens. Matter*, 1992, **46**, 11277.
29 A. I. Lebedev, I. A. Sluchinskaya, V. N. Demin and I. Munro, *Phys. Solid State*, 1999, **41**, 1275.
30 S. Ahmad, K. Hoang and S. D. Mahanti, *Phys. Rev. Lett.*, 2006, **96**, 056403.
31 M. Lach-hab, D. A. Papaconstantopoulos and M. J. Mehl, *J. Phys. Chem. Solids*, 2002, **63**, 833–841.
32 S. H. Wei and A. Zunger, *Phys. Rev. B: Condens. Matter*, 1997, **55**, 13605.
33 D. Parker and D. J. Singh, *Phys. Rev. B: Condens. Matter Mater. Phys.*, 2010, **81**, 195217.
34 J. P. Heremans, "The Effect of Resonant Energy Levels on the Thermoelectric Power and Thermoelectric Power Factor", Ch. 12 in *CRC Handbook on Thermoelectricity*, D. M. Rowe, Editor, 2011, (in Press).
35 J. Androulakis, C. H. Lin, H. J. Kong, C. Uher, C. I. Wu, T. Hogan, B. A. Cook, T. Caillat, K. M. Paraskevopoulos and M. G. Kanatzidis, *J. Am. Chem. Soc.*, 2007, **129**, 9780–9788.
36 A. J. Minnich, M. S. Dresselhaus, Z. F. Ren and G. Chen, *Energy Environ. Sci.*, 2009, **2**, 466–479.

